Innovative manufacturing processes for sustainable and more efficient manufacturing

Benjamin Peeters, Natalie Chernovol, Sylvie Castagne, Bert Lauwers

KU Leuven, Department of Mechanical Engineering and Flanders Make@KU Leuven-MaPS
Celestijnenlaan 300B, 3001 Heverlee (Leuven), Belgium

Abstract

Today's increasing demand for sustainable and more efficient manufacturing drives the development of innovative manufacturing processes. This paper describes the results of three research topics, performed on DMG MORI NTX2000 and DMU50 machining centers loaned by the MTTRF foundation to KU Leuven, aimed to achieve these goals. The first research topic of this paper focusses on surface hardening of mould components in two different tool steels (Stavax ESR, Sverker 21), using a selective laser hardening set-up integrated into the turn-mill center (DMG MORI NTX2000). Microhardness measurements showed a maximum achieved hardness of 614HV for Stavax ESR and 810HV for Sverker 21 respectively. The second topic focusses on the cutting performance of newly developed niobium carbide-based cutting inserts. The third topic deals with the post-machining of parts made by Wire and Arc Additive Manufacturing (WAAM). Multiple wall shaped samples with different WAAM parameters were produced and post-processed to optimized welding parameters during WAAM allowing to control the material usage more efficiently and reduce overall machining time.

Keywords: Scanning laser hardening, Niobium carbide, Tool wear, Wire and arc additive manufacturing (WAAM)

1 INTRODUCTION

More and more manufacturing organizations today recognize the trend towards sustainable and more efficient manufacturing is becoming an integral part of the way a product is produced, marketed, and purchased. To respond to this trend, research at KU Leuven aims the development of novel manufacturing processes that can achieve these goals. In this paper, three research topics are investigated.

The first topic focusses on the surface hardening of mould materials and components using a selective laser hardening set-up integrated into a turn-mill center. Integrated laser hardening has several advantages over conventional hardening techniques. Due to the elimination of large energy-consuming furnaces, the introduction of laser hardening lowers environmental impact compared to conventional hardening. Besides, the laser hardening process is a self-quenching process that does not require water or oil reducing the environmental footprint of the process. The (cooler) material around the laser hardened processing zone is sufficient to support the martensitic transformation [1]. In addition, laser hardening, often done in a selective manner, only heats the workpiece locally, avoiding large deformations. This results in a minimum number (often none) of hard finishing operations. In this paper, two materials commonly used in the injection moulding industry, Sverker 21, a high alloyed tool steel, and Stavax ESR, a stainless mould steel are studied. The development of the integrated scanning laser head, implemented within the DMG MORI NTX2000, has been discussed in earlier papers [2,3].

The next research topic focusses on the cutting performance of newly developed niobium carbide-based cutting inserts. Pressure on the manufacturing industry to find alternatives for the widely used Tungsten-Carbide Cobalt inserts are increasing. Oxides formed with both tungsten and cobalt are hazardous for human health. On the other hand, the pressure to reduce the use of cutting fluids during machining, for economic and environmental reasons, in the industry does imply a shift towards inserts that retain hardness and toughness better at elevated temperatures. A study performed by Woydt M. at all [4] indicated that NbC-Co retains hardness better at higher temperatures, and even surpasses the hardness of WC-Co grades above 700°C. At KU Leuven, two Niobium carbide-based cermets as an alternative to replace the Tungsten and Cobalt inserts in dry machining were developed. In this paper, the dry cutting performance of these two newly developed Niobium carbide-based cermets are compared to a commercial TiCN-Ni insert and a WC-Co coated inserts.

The last research topic focusses on the machining (finishing) of parts made by Wire and Arc Additive Manufacturing (WAAM). WAAM is an additive manufacturing technique that uses an electrical arc as a fusion source to melt a wire and deposit metal in a layer by layer manner. WAAM is one of the most promising techniques for manufacturing medium and large scale metal structures as it has relatively high deposition rates (1-4 kg/h), higher material (up to 90%), and energy efficiency compared to other metal Additive Manufacturing techniques. WAAM can reduce the part cost by reducing material wastage and time to market. Furthermore, it increases the design freedom of a part, which potentially results in the weight-saving of the final product. However, one of the main drawbacks of the WAAM is its low dimensional accuracy and surface quality (waviness $\approx$ 0.5 mm) that leads to the necessity of further post-processing using conventional subtractive techniques (i.e. milling, turning, etc.). In this research, multiple wall shaped samples with different WAAM parameters were produced and post-processed (machined). The goal is to find optimized WAAM (welding) parameters allowing to control the material usage more efficiently and reduce the overall machining time of a component.

2 SELECTIVE LASER HARDENING OF INJECTION MOULD COMPONENTS

Scanning laser hardening is used to uniformly harden surfaces wider than the maximum spot size of the laser beam. Research described in [5,6] illustrates that a softening effect occurs when hardening surfaces with multiple laser tracks adjacent to each other, caused by the annealing of the previous laser track beside the following track. This results in a non-uniform hardness across the hardened zone. To prevent annealing and to achieve a uniform hardened zone, Qui et al. [7] proposed to implement a scanning motion of the laser beam by deflecting it using a mirror mounted on a voice

coil. In this paper, a laser head set-up has been implemented on a DMG MORI NTX2000 Mill-turn center, where the potential of laser hardening has been proven by the research group [8]. The laser beam performs an oscillating movement by the integration of a voice coil mounted mirror (Figure 1a and 1b). The laser source used in this setup is a continuous-wave 500W diode laser with a wavelength of 940 nm. The laser head outputs a laser beam with a tophat laser profile at a minimal spot-size of 0.8mm.

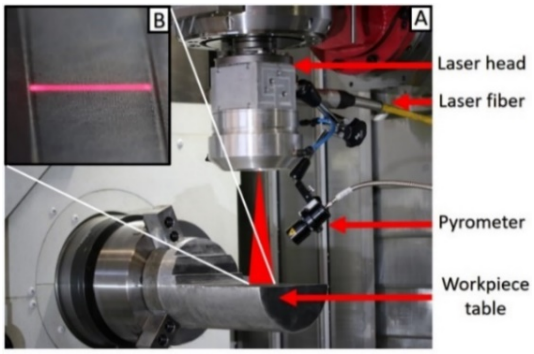

Figure 1: (a) Integration of a laser hardening tool within a DMG MORI NTX2000 machining center. (b) Scanning motion of the laser.

2.1 Material compositions and hardness

In co-operation with industrial partners, two types of tool steel alloys were selected: (1) Sverker 21 (SAE grade number 1.2379, with a chemical composition of 1.55% C, 0.3% Si, 0.4% Mn, 11.3% Cr, 0.8% Mo, 0.8%V) having a very good abrasive wear resistance and an initial hardness of 230HV; (2) Stavax ESR (SAE grade number 1.2083, with a chemical composition of 0.38% C, 0.9% Si, 0.5% Mn, 13.6% Cr, 0.3% V) used for small and medium inserts and cores, and an initial hardness of 210HV.

2.2 Experimental procedure

To find optimal parameter sets for laser hardening of Sverker 21 and Stavax, a sequence of tests is performed on milled bars of both materials with an average Ra of 0.28µm and a thickness of 10mm. An optimal parameter set is defined as a set of process parameters (in this research laser power, feed rate, scanning frequency) giving the highest hardness and highest hardening depth without signs of melt or deformation. This is done by gradually lowering the feed rate and/or scanning frequency at a fixed power until signs of melt are visually detected. Each hardness measurement is an average of three different measurements at the target location. The maximum hardness is the maximum hardness measured starting from 50µm below the surface of the sample. The hardness on the top surface of the samples can be higher than the maximum measured hardness. The hardening depths are measured on the cross-section of the hardened zone.

2.3 Results and discussion

2.3.1 Flat bars of Sverker 21 and Stavax

The scanning widths of a hardened zone has a significant influence on the achievable hardening depth. Laser scanning widths allow the material to dissipate the localized heat input faster than smaller scanning widths resulting in smaller hardening depths. But, it has also been observed that increasing the laser power to achieve bigger hardening depths with larger scanning widths result in melt and deformations of the surface of the samples. In this research three different scanning widths, 5mm, 18mm, and 30mm were tested. Initial experiments showed that keeping the laser power at 500W (maximum power of the set-up) at a spot size of 0.8mm yields the best results. During laser scanning, the laser spot moves at high speeds over larger areas requiring high laser powers. A scanning width of 30mm requires much slower scanning frequencies and feed rates than a scanning width of 5mm to harden a surface. On the other hand, fast scanning frequencies and feed rates are required for scanning widths of 5mm to prevent melting and deformations.

Figure 2 shows the result of the best samples tested for each scanning width. The results show that higher hardening depths can be achieved for smaller scanning widths for both Sverker 21 and Stavax. For Sverker 21 a scanning width of 5mm achieves a hardening depth of 0.4mm which is 1.6 times higher than with a scanning width of 30 mm. For Stavax a hardening depth of 0.2mm is achieved with a scanning width of 5mm. This is 4 times higher than the achieved hardening depth with a scanning width of 30mm. For Stavax the maximum available laser power of 500W is not sufficient to harden a width of 30mm deeper than 0.04mm. The scanning widths have no significant effect on the maximum hardness.

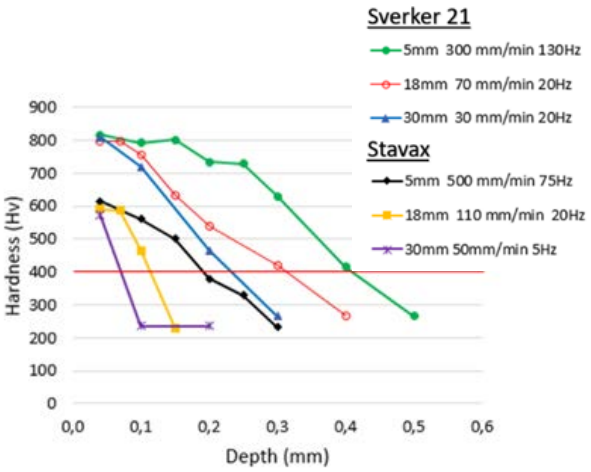

Figure 2: Hardness profile for Sverker 21 and Stavax for scanning laser hardening.

2.3.2 Industrial case: textured mould

Plastic components have a huge array of look and feel due to their surface texture. Texturing is achieved by adding a pattern to the molding surface of a mould. This allows the mould to transfer that pattern on each moulded part. Extensive use of these moulds will wear-off these textures resulting in parts with a different outlook and feel than originally intended. In this research, scanning laser hardening is used to harden textures (Figure 3a) of a Stavax mould for light switches without deforming the texture itself. The hardened mould has a texture that makes the surface of the lightswitch feel soft. The mould is prehardened to a hardness of 509HV. Initial testing showed that an oxidation layer, shown in Figure 3b, is formed on top of the hardened layer which cannot be removed without damaging the underlying texture. Different kinds of acids and oxidation removers (Oxalic acid, Sulfuric acid, HCL + H2O +

(CH2)6N4) were tested, but the oxidation layer remains attached unto the surface.

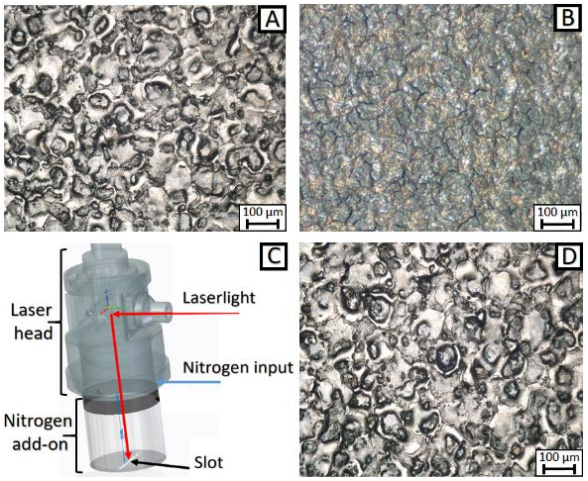

Figure 3: (a) Texture before laser hardening. (b) Oxidation layer after laser hardening. (c) Inert gas add-on. (d) Texture after laser hardening with nitrogen.

To prevent the creation of an oxidation layer, an inert gas add-on was designed to attach to the laser head. This add-on creates an inert environment at the location of the heat treatment. The inert gas add-on (Figure 3c), consists of a plexiglass tube covered with an aluminum plate. The inert gas is pumped into the plexiglass tube and is released through a slot in the aluminum plate the size of the maximum scanning width of the laser head. This add-on allows the inert gas to be applied at the exact location of the hardening. As shown in figure 3d no oxidation layer is visible on the textured mould after laser hardening the mould with nitrogen gas. Extensive tests proved a feed rate of 50mm/min, a power of 500W, a scanning width of 25mm at a scan frequency of 5 Hz generated the best results to harden these textures. Visually no changes in the textures were observable. The average Ra values (based on three locations and three repetitions) before laser hardening was 3.11µm and after laser hardening 3.17µm. The achieved hardness at a depth of 0.065mm is 615HV which is 106HV higher than the conventional hardened mould. The depth of 0.065mm is deep enough to through harden the whole texture.

3 CUTTING PERFORMANCE OF NIOBIUM CARBIDE-BASED CUTTING INSERTS

In this research, two newly developed niobium turning inserts are tested under dry cutting conditions and compared to a commercial TiCN-Ni insert and a WC-Co coated insert (Figure 4).

Figure 4: (a) Turning of C45 bars (DMG MORI NTX2000). (b) Geometry of tested inserts.

The first niobium insert, called C8, has the following chemical composition: 12Ti(C7N3)-40Ti(C5N5)-10NbC-7Co-7Ni-20WC-4Mo2C (wt%) the second insert, called C5, consists of 14TiC7N3-53NbC-9Ni-24WC (wt%). All tested inserts have an insert geometry according to ISO code TNMG160404R shown in Figure 4b. The tool life tests were performed on C45 bars cut to a length of 250mm with an initial diameter of 100 mm, shown in Figure 4a. The tool wear and workpiece surface roughness are both monitored.

3.1 Tool-life criteria and tool wear measurements

To assess the tool wear of the inserts, a 3-megapixel digital USB microscope with a magnification of 200x is used. This microscope is installed inside the machine and measures the tool wear at specific time intervals. According to the norm “Tool-life testing with single-point turning tools”, the width of the flank wear is the only tool-life criterion for these types of inserts. At each time interval, the average value of the flank wear at 3 separate locations is recorded (shown in red in Figure 5).

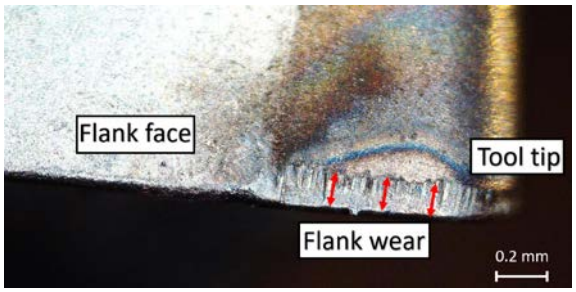

Figure 5: Flank wear measurement.

Figure 6 shows the flank wear of all 4 inserts at a cutting speed of 400m/min with a feed rate of 0,2mm/rev and depth of cut of 1mm. Flank wear of 0,150mm, indicated by the red line in Figure 6, was set as the maximum allowed flank wear. As shown in Figure 6, insert C5 shows the poorest performance, it reaches the maximum allowed flank wear of 0,150mm after 100s of machining. Both commercial inserts show comparable flank wear at 400s of machining but the flank wear of the TiCN insert propagates slower than the flank wear of the Wc-Co insert.

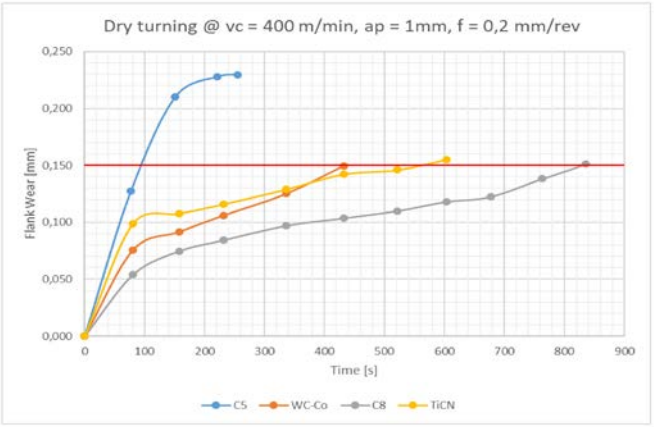

Figure 6: Flank wear of tested inserts.

The C8 insert shows the most promising results, outperforming the WC-Co insert by over 100% and the commercial TiCN insert by over 35% at the maximum allowed flank wear of 0,150mm. The most significant difference between the C5 and the C8 insert is the mass fraction of NbC. We can conclude that the 10%Nbc mass fraction in the C8 insert yields better results than the 53% NbC mass fraction in the C5 insert.

3.2 Roughness measurements

To compare the surface quality achieved by each insert, roughness measurements were performed at the same time intervals as the flank wear measurements. The roughness profile is measured at three randomly selected places on the workpiece surface. A cut-off wavelength λc of 2,5 mm was used with an evaluation length of 12,5mm. The average values of these three measurements are plotted in Figure 7.

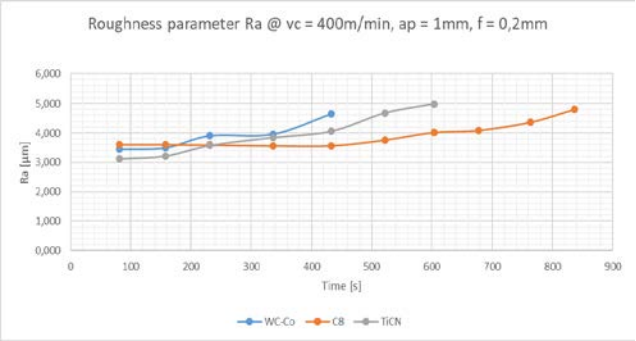

Figure 7: Surface roughness (Ra) of turned surfaces.

As expected a rising trend in roughness is observed with machining time. The roughness measurements of the C5 turned surfaces are left out since this insert produced inconsistent roughness throughout the turning passes with roughness values significantly higher than those machined with the other inserts. All 3 tested inserts initially produced similar roughness values, but as the turning time increases it is clear that the C8 insert produced the best results. If we correlate the flank wear measurements with the roughness measurements we observe that less flank wear produces smoother workpiece surfaces. Other types of tool wear were also present. Figure 8 shows all the tested tools once the tool-life criterion was reached.

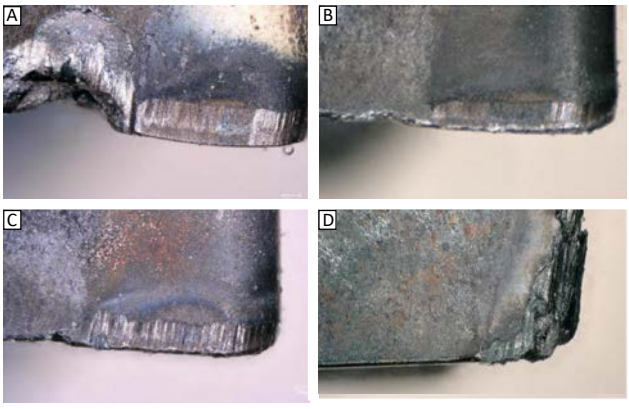

Figure 8: Tool-wear after reaching tool-life criterion. (a) C5 insert. (b) C8 insert. (c) TiCN insert. (d) WC-Co insert.

As can be seen in Figure 8a, the C5 insert suffered severe notch wear, indicating a low fracture toughness at elevated temperatures. The C8, shown in Figure 8b and commercial TiCN insert, shown in Figure 8c, both showed the same moderate amount of notch wear. The C8 however, took 35% longer to get the same amount of chipping and flank wear. The C8 insert seems to have both superior hot hardness and hot toughness compared to the commercial TiCN insert. The WC-Co insert showed no signs of notch wear. This insert failed due to a fractured of the tooltip shown in Figure 8d.

4 ADDITIVE-SUBTRACTIVE MANUFACTURING WITH WAAM

In this research Wire and Arc Additive Manufacturing (WAAM) with gas metal arc welding is used to produce wall shaped parts (Figure 9a). Due to the low dimensional accuracy and surface quality of the WAAM process, post-processing of the parts using conventional subtractive techniques is necessary. To achieve a geometrical and dimensional accurate part after post-processing, a sufficient amount of stock material, total wall width (TWW), is required. After the removal of the stock the EWW, the maximal wall width that can be obtained after post-processing for a specific set of WAAM process parameters, is obtained (Figure 9b). Previous experiments were conducted to build an empirical model to predict the geometry of one WAAM bead. The geometry of one bead depends on the wire feed speed (WFS) and travel speed (TS). Based on this empirical model a dimensional and geometrical accuracy of the final product can be estimated.

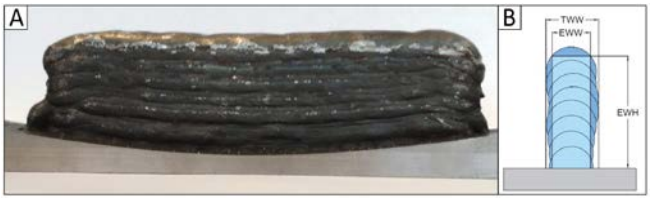

Figure 9: (a) Wall parts produced by WAAM. (b) Schematic representation of Effective Wall Width (EWW), Total Wall Width (TWW), and Effective Wall Height (EWH).

The post-processing steps of the parts consist of following steps: part digitalization (3D scanning), fitting of the reference CAD model within the actual component, alignment, subtractive process preparation in CAM software, and finally machining of the WAAM part. However, experiments showed that hidden undercuts still can be present in the parts. 3D scanning of the part does not provide sufficient information to detect all the undercuts in the part as EWW varies through the length of the component. Therefore, possible defects have to be determined after post-processing.

4.1 Preparation of WAAM samples

The parts were produces using a synergic controlled Qineo pulse 450A welding machine that is connected to a CLOOS QRC320H robot cell. This robot cell consists of a standard industrial 6-axis robot arm and 2-axis rotary table. The sample parts are built on a 30x10x200 mm mild steel base plates. To build up the wall layer by layer a 1.2 mm diameter weld wire EN ISO 14341-A (G 42 3 M21 3Si1) was used. This in combination with a shielding gas consisting of a mixture of 85% Ar with 15% CO2 at a constant flow rate of

15 l/min. The contact tip to work distance (CTWD) was equal to 15mm and was kept constant during deposition. As the relationship between the welding parameters and bead geometry is not linear, it is expected that the model for EWW prediction will also be non-linear. Therefore, a central composite design (CCD) was used to design the experiment. The WAAM process parameters and their limits are given in Table 1.

Table 1: WAAM process parameters and their limits.

Parameter	Factor levels				
	Level 1	Level 2	Level 3	Level 4	Level 5
WFS, m/min	2.5	2.9	3.8	4.6	5
TS, cm/min	15	22	38	53	60

The heat input during the WAAM process introduces significant angular distortions of the base plate (Figure 11a). These deformations lead to poor clamping and low alignment accuracy. To solve these problems the substrate plate is pre-machined after the WAAM process (Figure 11b). Pre-machined samples were scanned using an ATOS Compact 3D scanner. First, the scanned parts are aligned using the pre-machined surfaces of the substrate plate. Then, the dimensions of the scanned component were measured and a reference CAD model was created for every set of welding parameters. Further, the reference CAD model was fitted into the scanned component (Figure 10a). After the model fitting and alignment, the scanned component was exported and used as a blank in a CAM software to program the required milling steps (Figure 10b).

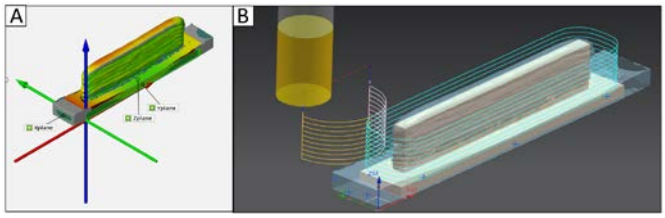

Figure 10: (a) Model fitting and alignment analysis. (b) Programming of the milling steps in CAM software.

4.2 Machining of wall parts

Machining was performed on a DMU 50 milling machine using a solid carbide end mill with a diameter of 20mm and 4 cutting edges. The parts were milled in 3 steps: roughing, semi-finishing, and finishing. Allowances for roughing and semi-finishing steps were determined from the 3D scan analysis. The finishing operations were programmed in multiple steps. After each finishing step, the surface of the milled wall was visually evaluated and a decision about the necessity of further machining was made (Figure 11c and d). The cutting parameters for each step are shown in Table 2 (a_e is the radial depth of cut and a_p axial depth of cut). After completing the EWW was measured with a micrometer.

Table 2: Cutting parameters for each step.

Step	S, rpm	F, mm/min	a_e, mm	a_p, mm
Roughing	4400	2700	0.5	3
Semi-finishing	4400	1080	0.2	3
Finishing	4400	1080	0.1	3

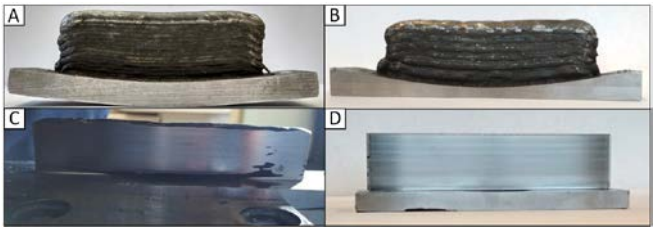

Figure 11: (a) deposition. (b) pre-machining of the substrate. (c) roughing and semi-finishing steps. (d) finishing step.

4.3 Results and discussion

To determine the relationships between the welding parameters and the maximum reachable EWW, a second-order regression model was used within the response surface method and is described by equation 1. The experimental design matrix and responses are provided in Table 3.

$$Y = \beta_0 + \sum_{i=1}^{k} \beta_i x_i + \sum_{i=1}^{k} \beta_{ii} x_i^2 + \sum_{i<j} \sum \beta_{ij} x_i x_j + \epsilon \qquad (1)$$

Table 3: Experimental design matrix and responses.

Sample	WFS m/min	TS cm/min	EWW mm	**Sample**	WFS m/min	TS cm/min	EWW mm
1	2.5	38	3.54	**8**	3.8	38	5.53
2	2.9	22	5.53	**9**	3.8	38	5.47
3	2.9	53	3.34	**10**	3.8	38	5.5
4	3.8	15	9.48	**11**	3.8	60	3.7
5	3.8	38	5.01	**12**	4.6	22	7.52
6	3.8	38	5.01	**13**	4.6	53	4.47
7	3.8	38	5.02	**14**	5	38	6.5

The response surface methodology was analyzed using Minitab software. Regular second-order regression models did not provide an adequate result with a lack-of-fit equal to 0.030. Therefore a Box-Cox transformation with $\lambda = -0.05$ was applied resulting in a lack-of-fit equal to 0.319 and an R^2 of 95.85%. The regression model for EWW determination is described by equation 2.

$$-\mathrm{EWW}^{-0.5} = -0.7232 + 0.1863 \cdot \mathrm{WFS} - 0.004034 \cdot \mathrm{TS} - 0.01844 \cdot \mathrm{WFS}^2 \qquad (2)$$

Using the response surface method a surface plot for EWW was obtained. The estimated minimal allowance to be removed from one side was calculated using models for EWW and bead width (W) and are determined by equation 3.

$$\text{Min allowance} = 0.5 \cdot (\mathrm{W} - \mathrm{EWW}) \qquad (3)$$

Based on Figure 12 (a) and (b) we can conclude that the travel speed during deposition has the most significant impact on the amount of stock to be removed during post-processing. Hence, TS values in a range of 35-60 cm/min in combination with WFS values less than 4.5 m/min are preferable for WAAM parts production. These results allow us to control the material usage more efficiently and reduce overall machining time by optimizing the welding parameters

during WAAM. These optimal welding parameters could be used not only for the production of a thin-walled component but also for solid structures deposited in a multi-pass multilayer way.

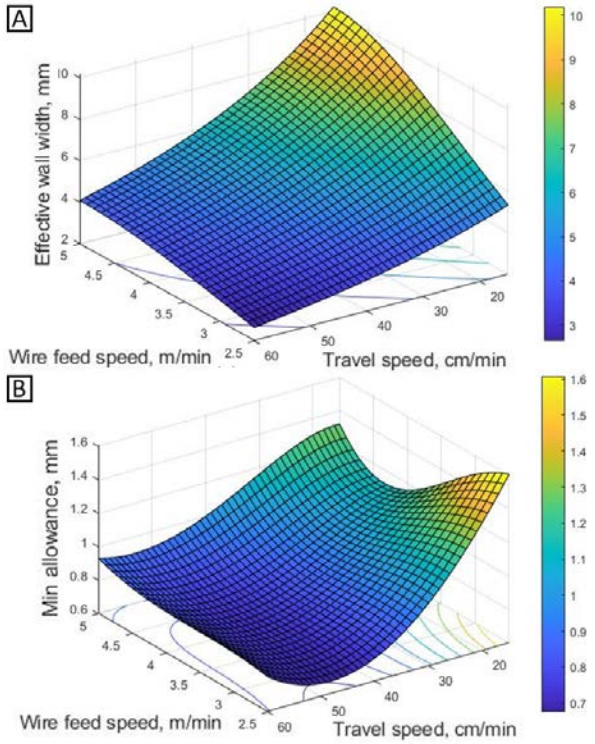

Figure 12: (a) Surface plot of EWW vs WFS. (b) Surface plot of estimated min allowance vs WFS and TS.

5 CONCLUSION AND OUTLOOK

The trend towards sustainable and more efficient manufacturing requires the development of innovative manufacturing processes. In this paper, three innovative processes, performed on a DMG MORI NTX2000 and a DMU50 machining centers loaned by the MTTRF foundation to KU Leuven, are investigated. The first research topic focuses on integrated scanning laser hardening of two materials used in the injection moulding industry, Sverker 21 and Stavax ESR. Using integrated laser hardening can significantly decrease the lead time and energy consumption of hardened components by eliminating the need for transportation and hard finishing of hardened components. The results of scanning laser hardening showed that higher hardening depths can be achieved for smaller scanning widths for both Sverker 2 and Stavax. Microhardness measurements showed a maximum achieved hardness of 614HV for Stavax ESR and 810HV for Sverker 21 after laser hardening. As a proof of concept, a textured mould was hardened. The texture mould could be hardened up to 615HV to a depth of 0.065mm without deforming the texture of the mould. The second research topic focuses on the cutting performance of newly developed niobium carbide-based cutting inserts. These Niobium carbide-based cermets can be alternatives to replace the hazardous Tungsten and Cobalt inserts for dry cutting conditions. Tool wear tests performed on C45 bars showed that the C8 insert containing 14TiC7N3-53NbC (wt%) outperforms a commercial WC-Co insert by over 100% and a commercial TiCN insert by over 35% at a maximum allowed flank wear of 0,150mm. Besides, the C8 insert also produces better Ra values on the surface of the machined bars. The C5 insert containing 14TiC7N3-53NbC (wt%) showed significantly faster flank wear compared to the C8, TiCN and WC-Co inserts. In the third research topic, Wire and Arc Additive Manufacturing (WAAM) is used to produce wall shaped parts. WAAM can produce large scale metal structures with lower material wastage and energy efficiency compared to other metal additive manufacturing techniques. In this paper wall shaped parts are produced and machined to optimizing the welding parameters during WAAM allowing to control the material usage more efficiently and reduce overall machining time. It can be concluded that TS values in a range of 35-60 cm/min in combination with WFS values less than 4.5 m/min are preferable for WAAM parts production.

ACKNOWLEDGEMENT

The authors would like to thank the Machine Tool Technologies Research Foundation (MTTRF) for supporting CNC Machining Centers to KU Leuven. The research has also been made possible through the financial support of the Flanders Agency for Innovation & Entrepreneurship (VLAIO) and this trough the projects INTLAS (IWT/150091/ICON, AdProcAdd (HBC.2018.0490) and the project NEXCER. This work was partially supported by KU Leuven Startfinanciering STG/18/026.

REFERENCES

[1] Dinesh Babu P., Buvanashekaran G., Balasubramanian K. R., Experimental investigation of laser transformation hardening of low alloy steel using response surface methodology, The International Journal of Advanced Manufacturing Technology 67, 2013, 1883-1897.

[2] Bouquet J., Peeters, B., Helsen, S., Mielnik, K., Lauwers, B., 2017, Programming and controlling the scanning laser hardening process, applied on complex shaped components on a Multi-axis Machining Center, Proc. MTTRF, San Fransisco,

[3] Peeters B., Bouquet J., Castagne S., Lauwers, B., 2019, Manufacturing of Components with a Hardened Top Layer on a Turn-Mill-Laser Center, Proc. MTTRF, San Fransisco,

[4] Woydt, M., Hyuang, S., Vleugels, J., Mohrbacher, H., & Cannizza, E. (2018). Potentials of niobium carbide (NbC) as cutting tools and for wear protection. International Journal of Refractory Metals, 380-387.

[5] Yao C., Xu B., Huang J., Zhang P., Wu Y., Study on the softening in an overlapping zone by laser-overlapping scanning surface hardening for carbon and alloyed steel, Optics and lasers in engineering, 2010, 20-26.

[6] Chaouch, D.; Guessasma, S.; Sadok, A. Finite Element simulation coupled to optimization stochastic process to assess the effect of heat treatment on the mechanical properties of 42CrMo4 steel. Mater. Des. 2012, 34, 679–684.

[7] Qui F., Kujanpä V., Surface hardening of AISI 4340 steel by laser linear oscillation scanning, Institute of materials, minerals and mining, 2012, 569-575

[8] Bouquet J., B. Peeters, O. Malek, G. Claus, P. Ten Haaf, A. Van Vlierberghe, B. Lauwers, Uniform hardening of steel components by integrated scanning laser hardening, 24th IFHTSE Congress, European Conference on Heat Treatment 2017